

## Characterization of ZnO Nanowire Field Effect Transistors by Fast Hydrogen Peroxide Solution Treatment

Taehyeon Kwon<sup>1\*</sup>, Woojin Park<sup>2\*</sup>, Minhyeok Choe<sup>2</sup>, Jongwon Yoon<sup>2</sup>, Sangsu Park<sup>2</sup>, Sangchul Lee<sup>1</sup>, Hyunsang Hwang<sup>1,2</sup>, and Takhee Lee<sup>3†</sup>

<sup>1</sup>Department of Nanobio Materials and Electronics, Gwangju Institute of Science and Technology, Gwangju 500-712, Korea

<sup>2</sup>School of Materials Science and Engineering, Gwangju Institute of Science and Technology, Gwangju 500-712, Korea

<sup>3</sup>Department of Physics and Astronomy, Seoul National University, Seoul 151-747, Korea

Received December 22, 2011; accepted January 15, 2012; published online March 1, 2012

This study demonstrates a simple and fast method of the operation mode control for ZnO nanowire field effect transistors (FETs) with hydrogen peroxide (H<sub>2</sub>O<sub>2</sub>, 10%) solution treatment for 5–10 s. With this H<sub>2</sub>O<sub>2</sub> treatment, the surface of ZnO nanowires was roughened as confirmed by transmission electron microscopy images and the defect level-related emission was increased from photoluminescence (PL) data. Correspondingly, the threshold voltage of H<sub>2</sub>O<sub>2</sub>-treated ZnO nanowire FETs shifted to the positive gate bias direction, leading a transition of the operation mode from depletion-mode to enhancement-mode. This H<sub>2</sub>O<sub>2</sub> solution treatment can be a useful method for controlling the operation mode of ZnO nanowire FETs with a wide threshold voltage shift in a few second solution treatment.

© 2012 The Japan Society of Applied Physics

### 1. Introduction

One-dimensional ZnO nanowires (NWs) are expected to be used for future electronic device applications such as light emitting diodes (LEDs),<sup>1)</sup> chemical sensors,<sup>2)</sup> photodetector,<sup>3,4)</sup> field effect transistors (FETs),<sup>5)</sup> logic circuits,<sup>6)</sup> and solar cells<sup>7,8)</sup> due to their unique properties such as a wide direct band gap (~3.4 eV) and a large exciton binding energy (~60 meV). Among these, the ZnO NW FETs are the fundamental element in the electrical devices. In particular, it has been investigated that the electrical properties of the NW FETs can be tuned by controlling interface morphology.<sup>9–11)</sup> Similarly, the electronic transport characteristics in NW FETs can be influenced by the surface morphology of the NWs which act as a channel of the FETs. We previously reported some ways for surface controlling of ZnO nanowires; surface of ZnO nanowires was modified by using different nanowire-growth substrates<sup>6,12)</sup> and solvent treatment with isopropyl alcohol (IPA).<sup>13,14)</sup> These methods could change the surface morphology of ZnO NWs and tuned the threshold voltages of NW FETs. For example, the surface morphology of the ZnO NWs was roughened by the IPA solution treatment technique and as a result, the threshold voltage of the IPA-treated ZnO NW FETs shifted toward the positive gate bias direction.<sup>13)</sup> However, in the case of IPA treatment, it takes long submersion time in IPA for longer period of time like about 30 days.<sup>13)</sup> Therefore, we have been looking for other solvents that can do the similar effects on the ZnO NW FETs but in much shorter treatment time.

In the present study, we investigated a simple and fast treatment method which controlled the threshold voltage of ZnO NW FETs by using hydrogen peroxide (H<sub>2</sub>O<sub>2</sub>) solution. The H<sub>2</sub>O<sub>2</sub> treatment caused the threshold voltage shift of ZnO NW FETs in a much shorter time of a few seconds. The ZnO NW FETs were submerged in 10% H<sub>2</sub>O<sub>2</sub> for three different periods: as-grown (no treatment), 5 s, and 10 s treatment. We observed that the change of surface roughness of ZnO NWs was occurred by the interaction between ZnO

NWs and the H<sub>2</sub>O<sub>2</sub> solution. The surface roughness induced more trapping of carrier electrons, causing electron depletion in ZnO NWs channel. As a result, the threshold voltage of the NW FETs shifted toward the positive gate bias direction and the operation mode converted from depletion-mode to enhancement-mode.

### 2. Experimental Procedure

ZnO NWs with smooth surface morphology were synthesized by a vapor transport method on an Au-coated *c*-plane sapphire substrate. The ZnO nanowires were grown on the substrates at 920 °C for ~25 min under a flow of Ar (50 sccm) and O<sub>2</sub> (0.2 sccm). Then, ZnO NWs were dispersed on a silicon substrate with a 100 nm-thick thermally grown SiO<sub>2</sub> layer to fabricate ZnO NW FETs. A silicon substrate and SiO<sub>2</sub> layer serve as a common back-gate electrode and a gate dielectric layer, respectively. Au/Ti source and drain electrodes were defined on an individual ZnO nanowire with a distance of 3 μm by photolithography, metal deposition, and lift-off processes. The more detailed growth of ZnO NWs and fabrication of ZnO NW FETs using a conventional back-gate configuration method has been reported elsewhere.<sup>10)</sup> To analyze and study the surface roughness control of ZnO NWs and their electrical performance, the FET devices were submerged in H<sub>2</sub>O<sub>2</sub>. Throughout this study, we used H<sub>2</sub>O<sub>2</sub> solution containing 10% hydrogen peroxide. Three conditions were prepared: as-grown, 5 and 10 s submersion time in H<sub>2</sub>O<sub>2</sub>. To systematically compare the electrical characteristics, the comparison was done on the same device for each condition. A JEM 2100F transmission electron microscope (TEM) and scanning electron microscopy (SEM) was used to investigate the surface morphology of ZnO NWs before and after the H<sub>2</sub>O<sub>2</sub> treatment. A Labram HR photoluminescence (PL) mapping system was conducted to study the optical properties of the ZnO NWs before and after the H<sub>2</sub>O<sub>2</sub> treatment. A semiconductor parameter analyzer (Agilent B1500A) was used to measure the electrical properties of the ZnO NW FETs at room temperature. In order to obtain statistical descriptions of the electronic transport characteristics of surface-roughened ZnO NWs, a total of 24 NW FETs were fabricated and submerged in H<sub>2</sub>O<sub>2</sub>.

\*These two authors contributed equally to this paper.

†E-mail address: tlee@snu.ac.kr

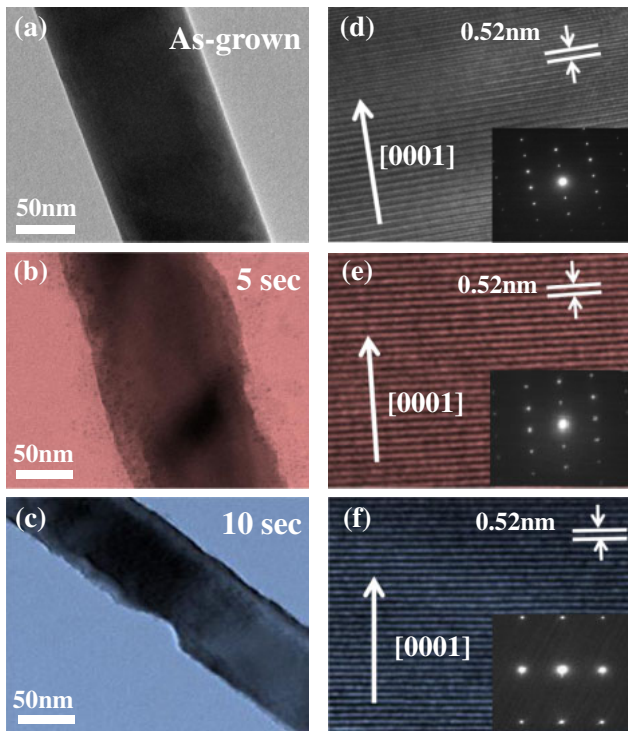


**Fig. 1.** (Color online) (a–c) Low-resolution TEM images and (d–f) HRTEM images of an as-grown ZnO nanowire (a, d), a ZnO nanowire with 10% H<sub>2</sub>O<sub>2</sub> for 5 s submersion (b, e), and 10 s submersion (c, f). The insets in (d–f) show the electron diffraction patterns.

### 3. Results and Discussion

Figures 1(a)–1(c) show low-magnification TEM images of ZnO NWs for as-grown and treated by H<sub>2</sub>O<sub>2</sub> submersion for 5 and 10 s, respectively. These images show the difference of the surface morphology between as-grown ZnO NWs and H<sub>2</sub>O<sub>2</sub>-treated ZnO NWs. It is clear that the surface of the 10 s treated ZnO NWs was rougher than that of the 5 s treated NW, and they were considerably rougher than the as-grown NWs. This result suggests that H<sub>2</sub>O<sub>2</sub> etched the surfaces of ZnO NWs and longer submersion time induced a rougher surface morphology. High-resolution TEM (HRTEM) images [Figs. 1(d)–1(f)] and the corresponding electron diffraction patterns (inset image) show that the NWs remained single crystalline regardless the surface roughness of the ZnO NWs treated by H<sub>2</sub>O<sub>2</sub>.

Figure 2(a) shows the PL spectra of the ZnO NWs with three different conditions; as-grown, 5- and 10-s-treated with H<sub>2</sub>O<sub>2</sub>. The ZnO NWs grown on the Au-coated *c*-plane sapphire substrate were transferred to Si wafers and 10 different positions were measured for PL characterization (for each sample). The PL emission consists of the ultraviolet (UV) emission band (left side, narrow band) and the defect level (DL)-related emission band (right side, broad band) associated with the surface defects of the NWs.<sup>15,16</sup> To clearly compare the DL emission intensity for each condition, the PL spectra were normalized by the UV emission intensity. From Fig. 2(a), the DL emission intensity of as-grown ZnO NWs was relatively weak compared to H<sub>2</sub>O<sub>2</sub>-treated ZnO NWs. In particular, this

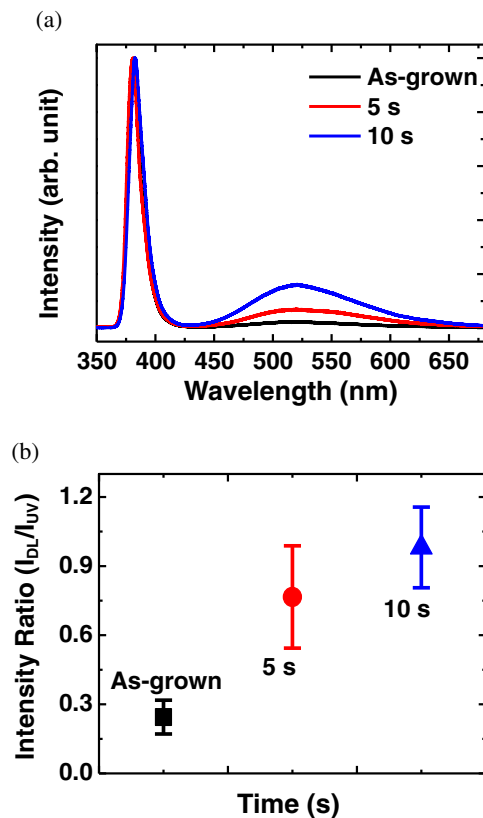


**Fig. 2.** (Color online) (a) PL spectra of the ZnO NWs and (b) the intensity ratios of I<sub>DL</sub>/I<sub>UV</sub> for three different conditions (as-grown, 5 s, 10 s) H<sub>2</sub>O<sub>2</sub> treatment.

DL-related peak increased for the ZnO NWs with longer H<sub>2</sub>O<sub>2</sub> treatment. Figure 2(b) is a statistical data of intensity ratios of DL emission peak to UV emission peak (I<sub>DL</sub>/I<sub>UV</sub>) for the as-grown and H<sub>2</sub>O<sub>2</sub>-treated (5 and 10 s) ZnO NWs. Because the DL emission peak is associated with surface defects of the crystal, the large I<sub>DL</sub>/I<sub>UV</sub> ratio means a large density of surface defects. As we can see in Fig. 2, the DL emission intensity and the intensity ratios were directly proportional to the process time in H<sub>2</sub>O<sub>2</sub>. Therefore, this observation indicates that the process time in H<sub>2</sub>O<sub>2</sub> affects the surface roughness.

To investigate the electrical properties of the ZnO NW FETs, three different conditions were prepared as similar to the studies of the surface roughness and PL data on the ZnO NWs. Figure 3(a) shows the transfer characteristics of the ZnO NW FETs (I<sub>D</sub>–V<sub>G</sub>, source–drain current versus gate voltage, at a fixed V<sub>D</sub> = 1 V) for the three different conditions; as-grown, 5 and 10 s in H<sub>2</sub>O<sub>2</sub> treatment. The measured threshold voltage of the as-grown ZnO NW FET was –27.05 V, and those of 5 and 10 s submersion times in H<sub>2</sub>O<sub>2</sub> were –7.33 and 7.98 V, respectively. Figure 3(a) indicates that the electrical transport properties of ZnO NWs were strongly influenced by H<sub>2</sub>O<sub>2</sub> treatment time. The as-grown ZnO NW FET had n-channel depletion-mode (D-mode) characteristics, which exhibits a negative threshold voltage. It means that the carriers are depleted in the conducting channel by applying a greater negative gate bias. On the other hand, the 10 s H<sub>2</sub>O<sub>2</sub>-treated FETs had n-channel enhancement-mode (E-mode) characteristics, ex-

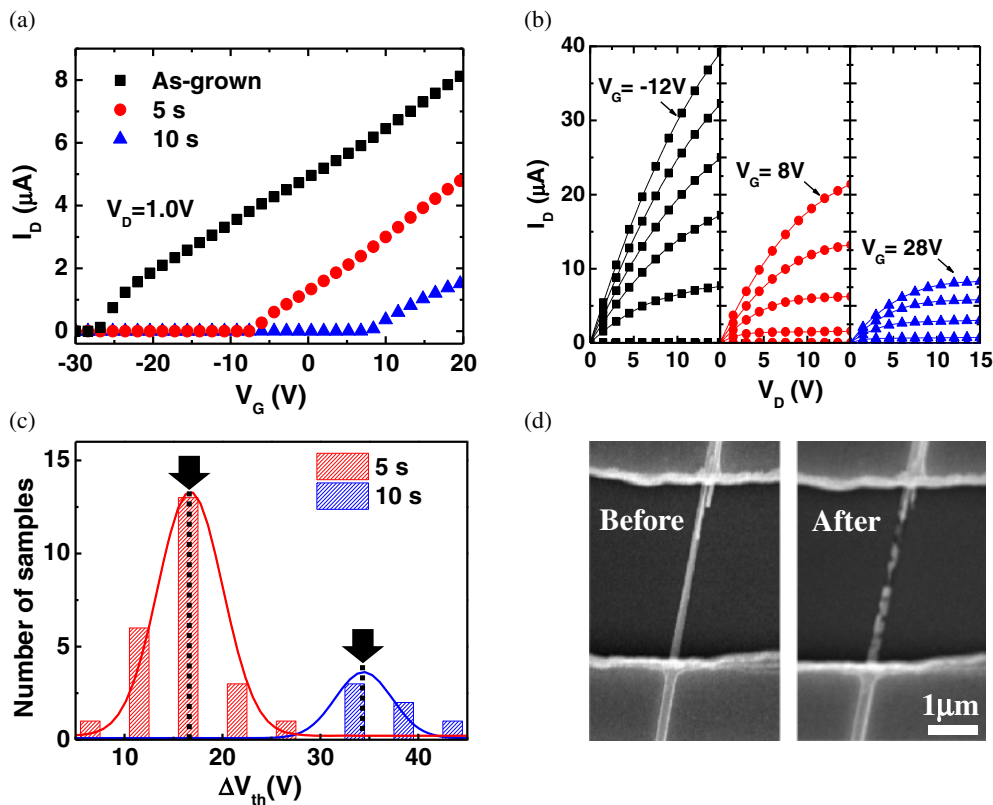


**Fig. 3.** (Color online) (a)  $I_D$ - $V_G$  curves and (b)  $I_D$ - $V_D$  curves of ZnO NW FETs measured before and after the  $H_2O_2$  treatment for 5 and 10 s. (c) Histogram and Gaussian fit of the threshold voltage shift of ZnO NW FETs with  $H_2O_2$  treatment for 5 and 10 s. (d) SEM images of ZnO NW before and after the  $H_2O_2$  treatment for 10 s.

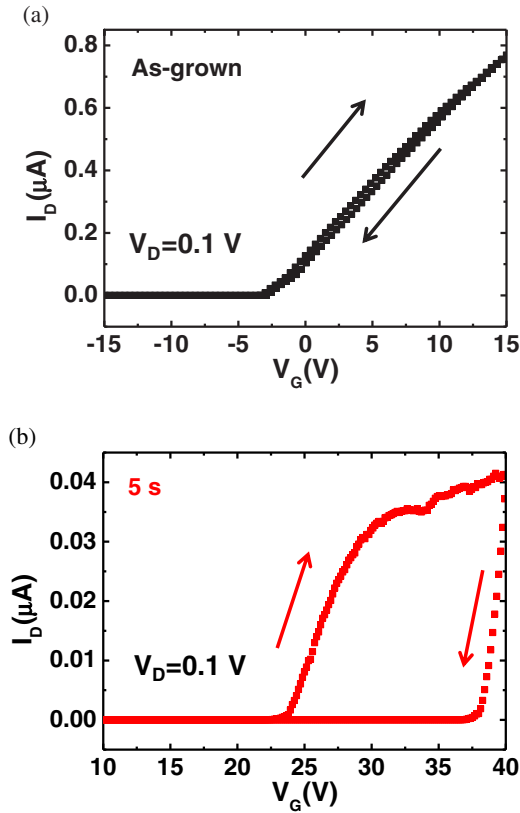
hibiting positive threshold voltage, which indicates that the carriers are generated in the conducting channel by applying a greater positive gate bias. Although the 5 s  $H_2O_2$ -treated NW FET was shifted by 19.72 V to the positive gate bias direction as compared to the as-grown ZnO NW FET case, it still maintained negative threshold voltage and D-mode characteristics. The results of Fig. 3(a) clearly demonstrate that the  $H_2O_2$  treatment could control the threshold voltage of ZnO NW FETs and tune the operation mode of the devices.

Figure 3(b) displays the output characteristics ( $I_D$ - $V_D$ , source-drain current versus source-drain voltage, at  $V_G = -12$ , 8, and 28 V) of the FETs for each condition. As shown in this figure, the drain current was reduced with increase of submersion time in  $H_2O_2$ , which is resulted to the threshold voltage shift phenomena [Fig. 3(a)]. Figure 3(c) shows the histogram and Gaussian fit of the threshold voltage shift of  $H_2O_2$ -treated ZnO NW FETs (5 and 10 s) as compared to the as-grown ZnO NW FETs. The average of the threshold voltage shift shown in Fig. 3(c) was extracted statistically from 24 FETs. The average value of the threshold voltage shift was found to be 17.0 and 35.5 V with 5 and 10 s submersion time in  $H_2O_2$  respectively. Note that only 8 out of 24 FET samples were observed for 10 s  $H_2O_2$ -treatment case because of the over-etching and damage caused by  $H_2O_2$  treatment. Figure 3(d) shows SEM images before and after a  $H_2O_2$  process for 10 s. This figure indicates that ZnO NW could be disconnected after 10 s submersion in  $H_2O_2$ . However, none of the devices died with 5 s  $H_2O_2$  treatment,

therefore, it would be important not to over-etch the ZnO NWs with  $H_2O_2$ .

The results of the observed roughened surface and the corresponding electrical properties of ZnO NWs with  $H_2O_2$  treatment can be understood by the following explanation. In relatively low concentration,  $H_2O_2$  annihilates oxygen vacancies existing on the ZnO NWs surface, i.e.,  $H + O^{2-} \rightarrow OH^- + e^-$ , and this results in increased-OH group concentration on the surface.<sup>11</sup> On the other hands,  $H_2O_2$  with relatively high concentration like 10% creates rougher ZnO NWs surface due to etching process. The surface scattering which is attributed to the roughened surface eventually overwhelms the opposite effect of the reduced surface oxygen vacancies. Surface defects on ZnO NWs serve as adsorption sites of  $O_2$  molecules<sup>17</sup> and these absorbed  $O_2$  molecules form  $O_2^-$  at defect sites and act as electron acceptors.<sup>17,18</sup> This reaction causes the depletion of electrons from the conduction channel, as a result, the source-drain current of the ZnO NW FET decreases and the threshold voltages of the device shifts towards the positive gate bias direction.

Figure 4 shows hysteresis behaviors for as-grown and  $H_2O_2$ -treated ZnO NW FETs. The hysteresis was more severe for the  $H_2O_2$ -treated ZnO NW FETs as compared to the as-grown ZnO NW FETs. This result was consistently observed in IPA-treated ZnO NW FETs.<sup>13</sup> The hysteresis of ZnO NW FET is attributed to the presence of adsorbed species.<sup>5</sup> A rough ZnO NW has much more adsorbed sites than a smooth ZnO NW, thus, there is a higher density of



**Fig. 4.** (Color online) Hysteretic behavior for (a) as-grown and (b)  $\text{H}_2\text{O}_2$ -treated ZnO NW FETs.

adsorbed species on a rough ZnO NW surface. As a result, charge trapping of carriers is more severe in a rough ZnO NW by the higher density of adsorbed species, showing a large hysteresis width. The clockwise hysteresis direction [Fig. 4(b)] may be explained by charge trapping and detrapping phenomena. When the back bias sweeps from negative bias, i.e.  $-20\text{ V}$ , initially trapped-electrons at the interface between the ZnO NW and  $\text{SiO}_2$  dielectric layer would be detrapped by Coulomb force and then become free carriers, inducing high current. On the other hand, when the back bias sweeps from positive bias, i.e.  $+20\text{ V}$ , some free carriers would be trapped at the interface between the ZnO NW and  $\text{SiO}_2$  dielectric layer, inducing reduced current value. Therefore, high current can be obtained for bias sweeping from  $-20$  to  $+20\text{ V}$ , while low current can be obtained for bias sweeping from  $+20$  to  $-20\text{ V}$ , showing clockwise sweeping direction, as shown in Fig. 4(b).

Figures 5(a) and 5(b) show the statistical data of the mobility and the subthreshold swing versus the processing time in  $\text{H}_2\text{O}_2$  (as-grown, 5 s, and 10 s) respectively. The mobility was calculated from the equation,  $\mu = g_m L^2 / V_D C_G$ , where  $C_G = 2\pi\epsilon_r\epsilon_0 L / \cosh^{-1}[(r+h)/r]$  is the gate capacitance. Here,  $g_m = dI_d/dV_G$  is transconductance,  $r$  is the NW radius ( $\sim 50\text{ nm}$ ),  $L$  is the NW channel length ( $\sim 4\text{ }\mu\text{m}$ ),  $h$  is the gate dielectric thickness ( $100\text{ nm}$ ),  $\epsilon_0$  is the permittivity of free space, and  $\epsilon_r$  is the dielectric constant of  $\text{SiO}_2$  (3.9). In Fig. 5(a), the average mobility values of ZnO NW FETs were found to be 81.3, 34.1, and  $12.9\text{ cm}^2\text{ V}^{-1}\text{ s}^{-1}$  for different conditions; as-grown, 5 s, and

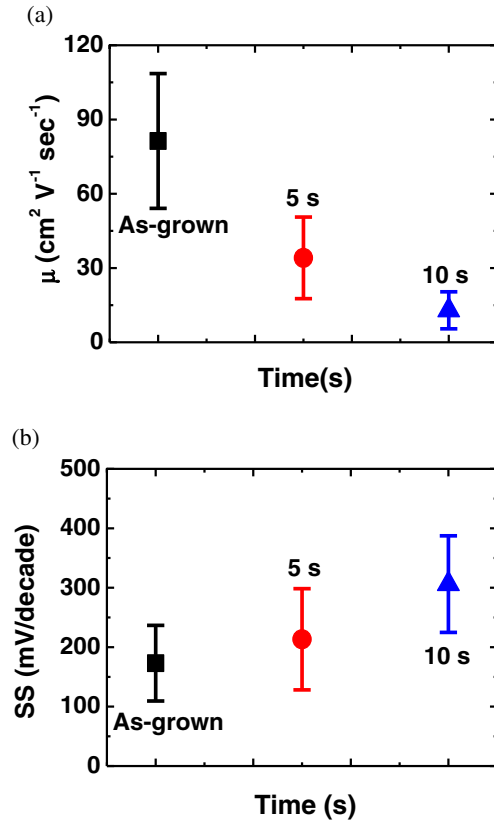


**Fig. 5.** (Color online) (a) Statistical distribution of the mobility ( $\mu$ ) and (b) subthreshold swing (SS) values as a function of the submersion time in  $\text{H}_2\text{O}_2$ .

10 s in  $\text{H}_2\text{O}_2$ , respectively. The longer submersion time in  $\text{H}_2\text{O}_2$ , the more surface defects are generated. Then, this causes more surface scattering, and draws more  $\text{O}_2$  molecules onto the ZnO NWs surface than as-grown ZnO NWs.<sup>11)</sup> The surface scattering reduces the carrier mobility, and relatively more  $\text{O}_2$  molecules on the ZnO NW FETs decreases the gate-couplings effect.<sup>12,19,20)</sup> The decrease of the gate-couplings effects increased the subthreshold swing (SS) as shown in Fig. 5(b).

#### 4. Conclusions

In summary, we studied the structural, optical, and electrical properties of ZnO NW FETs with the treatment of 10%  $\text{H}_2\text{O}_2$  solution for short process times (5 and 10 s). We observed that the submersion of ZnO NWs in  $\text{H}_2\text{O}_2$  roughened the surface morphology of NWs and increased the intensity ratio of the defect-related emission in PL spectra. Correspondingly, the threshold voltage of the  $\text{H}_2\text{O}_2$ -treated ZnO NW FETs shifted to the positive gate bias direction. As a result, the operation mode conversion from depletion-mode to enhancement-mode was achieved in ZnO NW FETs with this fast and simple  $\text{H}_2\text{O}_2$  solution treatment method.

#### Acknowledgments

This work was supported by the National Research Laboratory Program, the National Core Research Center grant, and the World Class University program from the Korean Ministry of Education, Science and Technology.

- 1) J. Bao, M. A. Zimmler, and F. Capasso: *Nano Lett.* **6** (2006) 1719.
- 2) Q. Wan, Q. H. Li, Y. J. Chen, T. H. Wang, X. L. He, J. P. Li, and C. L. Lin: *Appl. Phys. Lett.* **84** (2004) 3654.
- 3) J. Law and J. Thong: *Appl. Phys. Lett.* **88** (2006) 133114.
- 4) F.-S. Tsai, S.-J. Wang, Y.-C. Tu, Y.-W. Hsu, C.-Y. Kuo, Z.-S. Lin, and R.-M. Ko: *Appl. Phys. Express* **4** (2011) 025002.
- 5) J. Goldberger, D. J. Sirbully, M. Law, and P. Yang: *J. Phys. Chem. B* **109** (2005) 9.
- 6) G. Jo, W.-K. Hong, J. Maeng, M. Choi, W. Park, and T. Lee: *Appl. Phys. Lett.* **94** (2009) 173118.
- 7) M. Law, L. E. Greene, J. C. Johnson, R. Saykally, and P. Yang: *Nat. Mater.* **4** (2005) 455.
- 8) M. Liu and H. Kim: *Appl. Phys. Lett.* **84** (2004) 173.
- 9) D. Park, J. Lee, D. Kim, S. Mohanta, and H. Cho: *Appl. Phys. Lett.* **91** (2007) 143115.
- 10) S.-H. Park, S.-Y. Seo, and S.-H. Kim: *Appl. Phys. Lett.* **88** (2007) 251903.
- 11) Y. Hu, Y. Liu, H. Xu, X. Liang, L. Peng, N. Lam, K. Wong, and Q. Li: *J. Phys. Chem. C* **112** (2008) 14225.
- 12) W.-K. Hong, J. Sohn, D.-K. Hwang, S.-S. Kwon, G. Jo, S. Song, S.-M. Kim, H.-J. Ko, S.-J. Park, M. Welland, and T. Lee: *Nano. Lett.* **8** (2008) 950.
- 13) W. Park, W.-K. Hong, G. Jo, G. Wang, M. Choe, J. Maeng, Y. Kahng, and T. Lee: *Nanotechnology* **20** (2009) 475702.
- 14) W. Park, G. Jo, W.-K. Hong, J. Yoon, M. Choe, S. Lee, Y. Ji, G. Kim, Y. Kahng, K. Lee, D. Wang, and T. Lee: *Nanotechnology* **22** (2011) 205204.
- 15) I. Shalish, H. Temkin, and V. Narayanamurti: *Phys. Rev. B* **69** (2004) 245401.
- 16) H. Xue, N. Pan, R. Zeng, M. Li, X. Sun, Z. Ding, X. Wang, and J. G. Hou: *J. Phys. Chem. C* **113** (2009) 12715.
- 17) Z. Fan, D. Wang, P.-C. Chang, W.-Y. Tseng, and J. Lu: *Appl. Phys. Lett.* **85** (2004) 5923.
- 18) F. Chaabouni, M. Abaab, and B. Rezig: *Sens. Actuators B* **100** (2004) 200.
- 19) S. Song, W.-K. Hong, S.-S. Kwon, and T. Lee: *Appl. Phys. Lett.* **92** (2008) 263109.
- 20) O. Wunnicke: *Appl. Phys. Lett.* **89** (2006) 083102.